International Journal of Research in Engineering and Science (IJRES)
ISSN (Online): 2320-9364, ISSN (Print): 2320-9356
www.ijres.org Volume 13 Issue 8 ǁ August 2025 ǁ PP.160-171

Aerodynamic Development of an FSAE Undertray: CFD Analysis and Wind Tunnel Correlation

Shijaz Ahammed Afsal Kalathil
*[*1]Department of Aerospace engineering, Brunel University, London, United Kingdom*
Corresponding Author: Shijaz Ahammed Afsal Kalathil

Abstract
This thesis explores the design and optimisation of an undertray for a Formula SAE (FSAE) competition vehicle. The objective is to maximize aerodynamic efficiency, particularly focusing on downforce and drag reduction. The study begins with a computational approach using CAD software (On Shape) and Computational Fluid Dynamics (CFD) designing and simulation tools (ANSYS Fluent) to create and refine undertray designs. These designs are evaluated under different conditions to optimize airflow, reduce drag, and increase downforce for enhanced vehicle performance. To validate the findings, a scaled model of the undertray is 3D printed and tested in a wind tunnel, providing empirical data to complement the simulations. Insights and data from this testing are used to further refine the design, with an emphasis on compliance with the 2024 Formula SAE UK regulation. The project also pays homage to historical undertray designs, such as the Venturi tunnels and multi-deck diffusers, by integrating their lessons learned into the development of an innovative undertray for modern racing.
The final phase explores scaling the design for a Formula One car, considering the 2024 FIA regulations. This research offers a comprehensive methodology for bridging simulation and real-world testing, contributing valuable insights to motorsport aerodynamic design.
Keywords: *Aerodynamics, Undertray design, Computational Fluid Dynamics (CFD), Wind Tunnel Testing, Formula SAE(FSAE), Formula One regulations, Downforce and Drag Optimisation.*

Date of Submission: 14-08-2025 Date of acceptance: 28-08-2025

I.INTRODUCTION

In the high-stakes world of Formula One and Formula SAE racing, aerodynamic optimisation is critical for achieving peak performance. The undertray, a key aerodynamic component beneath the car, plays a vital role in generating downforce to enhance grip and stability, while minimising drag to improve speed and efficiency. Working alongside elements like the diffuser and wings, the undertray helps manage airflow and ground effect, particularly during high-speed cornering.

Historically, undertray designs have evolved from flat-bottomed setups to complex geometries that exploit advanced aerodynamic principles, all within the constraints of evolving FIA regulations. This project focuses on designing and optimising an undertray for Brunel University's FSAE team (BMM), using CAD (Onshape) and CFD tools (ANSYS Fluent) to simulate and refine airflow characteristics. A scaled 3D-printed model will undergo wind tunnel testing to validate simulation results.

The final phase explores scaling the optimised design for a Formula One application in line with the 2024 FIA rules. By combining simulation and empirical testing, this research aims to contribute meaningful insights into aerodynamic design for competitive motorsport.

II.METHEDOLOGY

2.1 Overview

This project follows a structured methodology to design, simulate, and test an aerodynamic undertray for Brunel Masters Motorsport's (BMM) Formula Student car. The process includes CAD modelling in Onshape, CFD simulations in ANSYS, physical prototyping via 3D printing, wind tunnel testing, and redesign for a full-scale Formula One application.

2.2 CAD Design and Initial Simulation

Using Onshape, a custom undertray was designed to fit the BMM Formula Student vehicle, tailored to its chassis constraints (560 mm width, 785 mm length). Key design goals included increasing downforce and reducing drag. Figures 11 and 12 illustrate the top and bottom views of the vehicle with the undertray.

Figure 1 top view of BMM vehicle

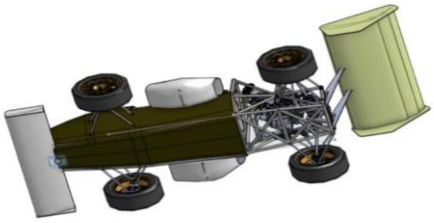

Figure 2 bottom view of BMM vehicle

2.3 Dimensioning and Regulatory Compliance

The design was verified against the 2024 Formula Student UK (FSUK) rules, including the 500 mm height limit for aero devices and a 250 mm maximum extension beyond the rear tires. These constraints guided the initial and final design (Figures 3 and 4), which was then prepared for simulation.

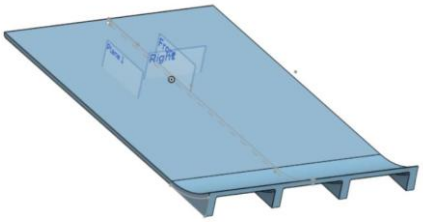

Figure 3 Initially designed Undertray (topview)

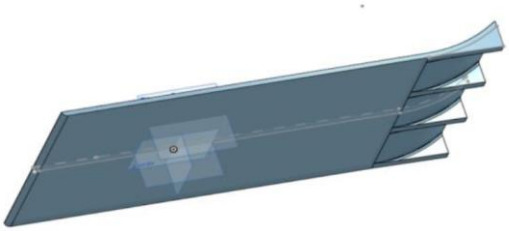

Figure 4 Initially designed undertray (Bottomview)

2.4 CFD Analysis

The initial undertray model was imported into ANSYS CFX, using the SST turbulence model for accurate boundary layer and separation analysis. Simulations were run at speeds of 15 m/s² and 28.5 m/s² with a 6.144 mm ground clearance, and boundary conditions matching wind tunnel conditions (19°C, 1008 kPa). Pressure and velocity contours (Figures 5 and 6) helped identify areas for aerodynamic improvement.

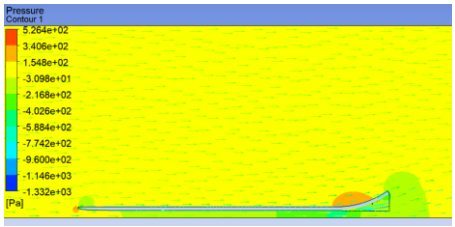

Figure 5.
ANSYS CFX Pressure contour at15m/s

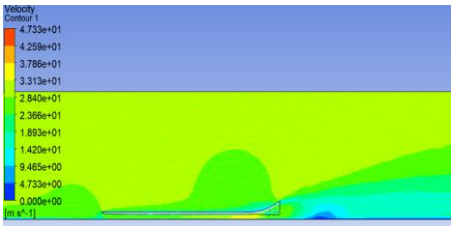

Figure 6 :
ANSYS CFX velocity contour at 15m/s

2.5 Design Optimisation Inspired by Formula One

To improve the aerodynamic performance of the initial undertray design, inspiration was taken from the 2021 Mercedes AMG Petronas Formula One Team's undertray, which prominently featured aerofoil-shaped channels and contoured surfaces for efficient airflow management (Figure 7). This design served as a benchmark for refining the BMM undertray, aiming to maximise downforce while minimising drag.

Figure 7.Undertray of 2021 Mercedes AMG Petronas Formula One Team

The original flat or mildly contoured surfaces of the BMM undertray were redesigned to include curved aerofoil profiles, which promote accelerated airflow under the car, lowering pressure in accordance with Bernoulli's principle and enhancing ground effect. These profiles were integrated particularly in the mid-section and diffuser area, encouraging smooth flow transition and improving pressure recovery toward the rear of the vehicle.

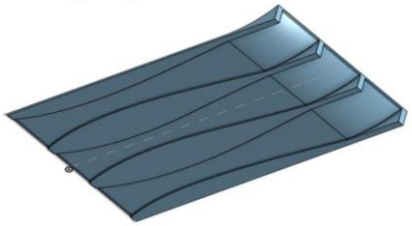

Figure 8. Final design of the BMM Undertray (bottom view)

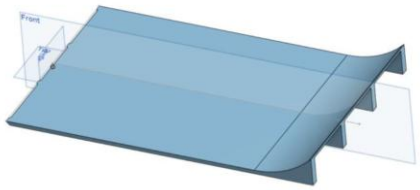

Figure 9. Final design of the BMM Undertray (top view)

The redesigned model (Figures 18 and 19) was simulated at multiple speeds (10–28.5 m/s²) and ground clearances (6.144 mm and 4.144 mm), showing improved aerodynamic efficiency than the initial undertray design (Figures 10 and 11).

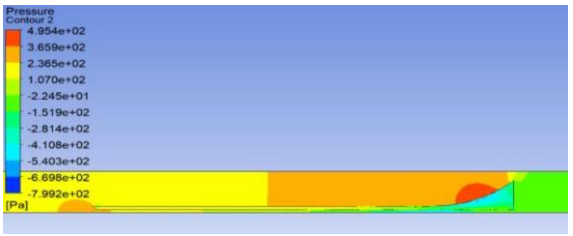

Figure 10. ANSYS CFX Pressure contour at 20ms (side view)

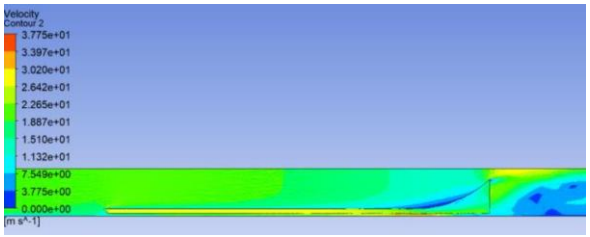

Figure 11. ANSYS CFX Velocity contour at 20ms (side view)

2.6 Scaling for Wind Tunnel Testing

To validate CFD results, a 1:5 scale undertray was created for wind tunnel testing. The scaled model (Figures 22 and 23) included features like pressure tap holes and removable lids. Initial ABS 3D prints (Figures 24 and 25) were too fragile, leading to multiple redesigns.

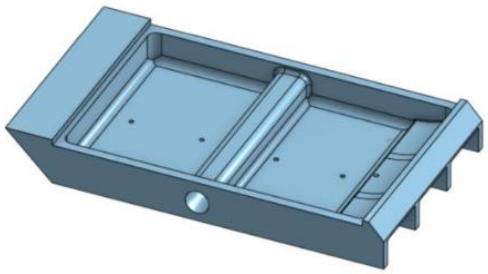

Figure 12: Scaled and redesigned model for Wind tunnel testing (Isometric bottom View)

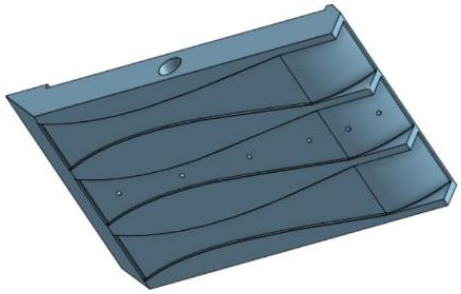

Figure 13: Scaled and redesigned model for Wind tunnel testing (Isometric Top View)

Figure 14: Failed Printed Model for Wind Tunnel Tests (isometric bottom view)

Figure 15. Failed Printed Model for WindTunnel Tests (side view)

2.7 3D Printing and Refinement

To improve strength and accuracy, resin printing was used. Resin offered smoother surfaces and better structural integrity. The model was refined by increasing wall thickness and reinforcing critical features like the mounting rod, which was enlarged from 2.5 mm to 5.5 mm (Figures 16,17).

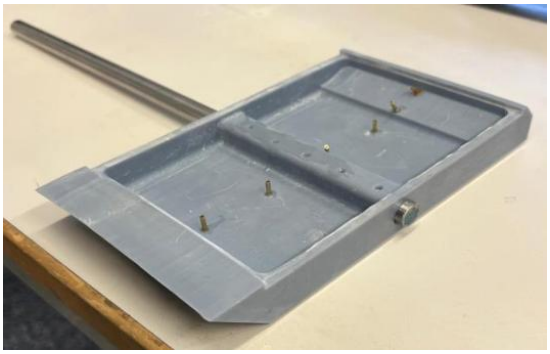

Figure 16: Resin printed Model with Pressure taps and Rod for Wind Tunnel Testing (isometric top view)

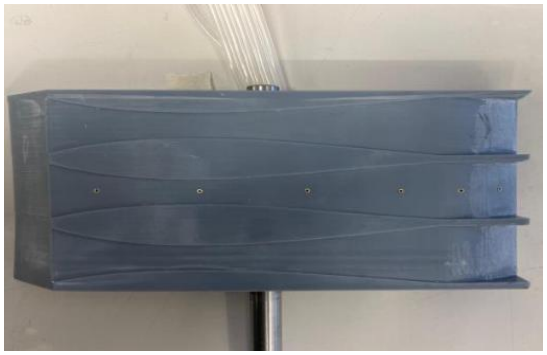

Figure 17.Resin printed Model (bottom view)

2.8 Pressure Tap Installation and Data Collection

Pressure taps were added to the undertray to measure local pressure variations during wind tunnel tests (Figure 29). These measurements provided empirical data to validate CFD results and assess aerodynamic performance.

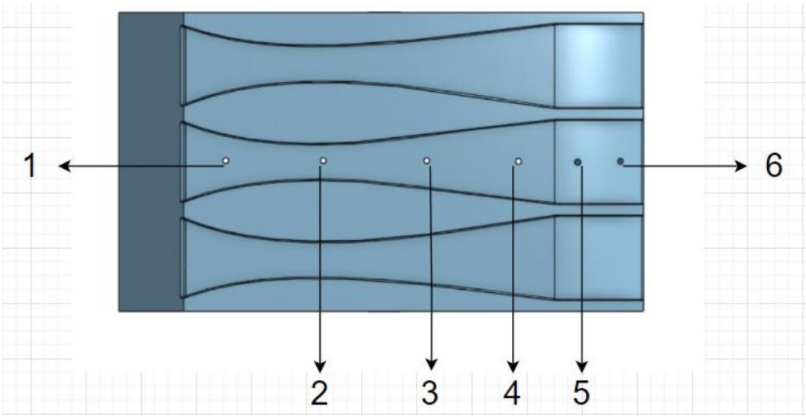

Figure 18. Pressure Tap Placement

2.9 Pressure Tap Placement

Taps were placed at key aerodynamic zones:

- **Tap 1**: Near the inlet, measuring initial airflow pressure
- **Tap 2**: In the convergent section, where airflow velocity increases
- **Taps 3–4**: Just after convergence, near the diffuser entrance
- **Taps 5–6**: Along the diffuser curve and exit, capturing pressure recovery

These placements were informed by CFD flow data and were critical in evaluating pressure gradients and diffuser effectiveness.

2.10 Wind Tunnel Operations

The AF1300 subsonic wind tunnel provides a controlled environment for aerodynamic testing. Air is drawn through a diffuser to accelerate and smooth the flow before entering the working section. A protective grill surrounds the variable-speed axial fan, followed by a second diffuser to stabilize airflow. Pressure is continuously monitored to maintain consistent testing conditions.

Figure 19 :AF1300 Wind Tunnel

Data collection occurs at high frequency: lift and drag forces are recorded every 5 seconds, while pressure data is captured every 2 seconds, enabling accurate analysis of aerodynamic behaviour.

2.10.1 Wind Tunnel Testing

The initial model, once printed and reinforced, was tested at 15 m/s and 28.5 m/s. It failed at the higher speed due to structural limitations, as shown in Figures 20 and 21.

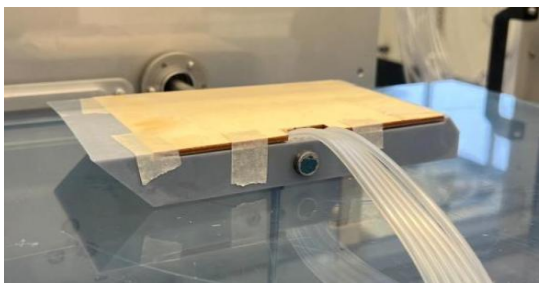

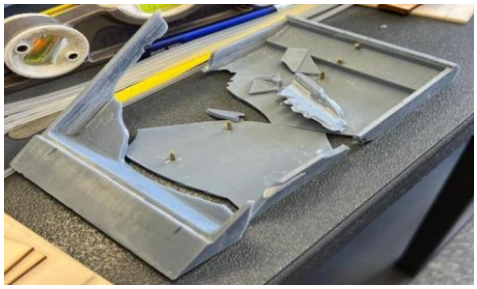

Figure 20 :Model Inside the wind tunnel (isometric view) figure 21.Model shown in a broken state after testing

To address this, the model was redesigned with thicker walls and stronger rod reinforcements. The updated model was then tested successfully at 10 m/s, 15 m/s, and 20 m/s, providing valuable lift, drag, and pressure data for undertray performance validation.

2.10.2 Ground Clearance Testing

Wind tunnel tests also investigated ground clearance effects, using scaled-down heights of 1.2 mm and 0.8 mm, equivalent to 6.144 mm and 4.144 mm on the full-scale car. These clearances reflect typical and lowered ride heights achievable via suspension adjustments. A flat glass plate (Figure 22) ensured consistent clearance during testing.

Figure 22 Flat glass plate for Setting ground clearance inside the wind tunnel

2.11 Designing the F1 Undertray

2.11.1 Real-World F1 Design Insights

The 2024 FIA Formula One Technical Regulations were studied to inform the F1 undertray design, referred to as "**bodywork facing the ground**" in the rulebook. These rules ensure safety and aerodynamic fairness by limiting flexibility and mandating strict geometry.

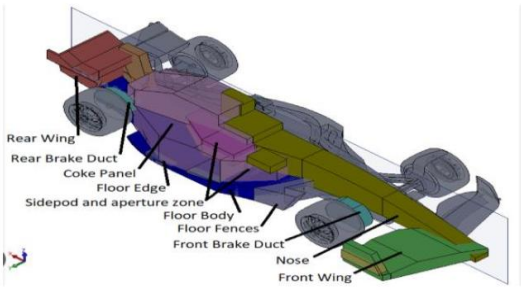

Figure 23 :Exterior parts of a Formula one car

Key components include:

- **Plank Assembly** (Jabroc): Controls ride height and centre of gravity.
- **Floor Body, Fences & Edge Wings**: Must follow surface continuity and volume constraints.

- **Bib & Floor Assembly**: Smooth transitions with regulated skids for protection.
- **Diffuser**: Generates downforce through controlled pressure differentials.
- **Auxiliary Components**: Support structures and sensor apertures, within geometric limits.

2.11.2 Model Design and Implementation

A full CAD model of the F1 undertray was created using **Onshape**, based on both FIA regulations and analysis of recent F1 cars (2023–2024). The focus remained solely on the undertray, excluding wings or suspension for simplicity. The final design (Figure 24) is regulation-compliant and aerodynamically optimized.

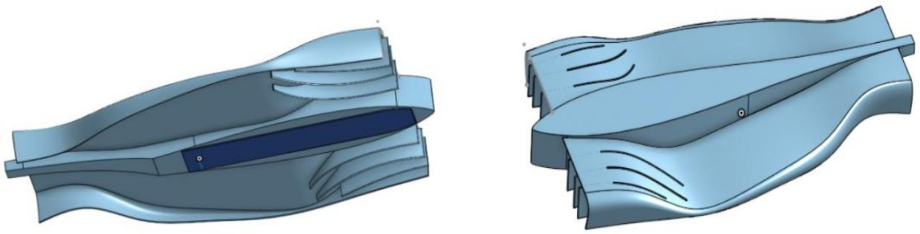

Figure 24 :Newly designed undertray for Formula one car

2.11.3 Model Limitations

Due to the complexity of the F1 undertray, the model exceeded the **500,000-node limit** of the ANSYS Student software after meshing. Despite efforts to reduce mesh density, the simulation couldn't proceed within the software's constraints, preventing full CFD validation of the F1 design

III Results and Discussion

3.1 CAD Design and Initial Simulation

The initial undertray aimed to improve downforce while keeping drag low, using a simple structure with a large rear diffuser. Simulations at 15 m/s and 28.5 m/s showed performance, with downforce increasing significantly at higher speeds:

Speed (m/s)	Drag Force (N)	Lift Force (N)
15	3.93	-26.25
28.5	14.37	-72.23

Table 1: Initial undertray Drag vs Lift values at ride height 6.144m

These results confirm that the basic design generated strong downforce with speed but left room for aerodynamic optimization.

3.2 Design Optimization Inspired by Formula One

Drawing inspiration from the Mercedes-AMG Petronas F1 team's 2021 undertray (figure 7), the BMM undertray model was redesigned with an aerofoil-inspired shape. Three closely positioned aerofoils were integrated beneath the tray to optimize airflow using the Venturi effect, streamlining air movement, reducing turbulence, and improving aerodynamic efficiency.

Re-simulation in ANSYS CFX showed a clear performance boost, with drag significantly reduced and downforce increased. A key objective was upholding mass conservation: ensuring the air entering the system matched the air exiting, preventing pressure build-up or loss.

This precise airflow management enhanced stability, grip, and handling, especially at high speeds and during cornering. The optimization highlights effective application of aerodynamic principles and advanced simulations, achieving notable performance gains.

3.3 Section-Wise Analysis of the Undertray: Venturi Effect and Bernoulli's Principle

The optimized undertray's airflow can be divided into three regions: inlet, centre, and outlet (refer figure(18). Together, they illustrate how the Venturi effect and Bernoulli's principle generate downforce and reduce drag.

- Section 1: Inlet (Low-Speed, High-Pressure)

Air enters between the aerofoils through a wider cross-section, moving slowly but at higher pressure. This controlled intake ensures steady airflow into the undertray.

- Section 2: Centre (High-Speed, Low-Pressure)

As air is compressed in the narrow middle section, velocity increases sharply and pressure drops. The resulting low-pressure zone creates suction, generating strong downforce and improving stability at high speeds.

- Section 3: Outlet (High-Speed, Stabilized Pressure)

The air exits through a widening cross-section, maintaining high speed while pressure stabilizes. This smooth transition reduces turbulence and drag, sustaining aerodynamic efficiency.

In summary, by accelerating and compressing airflow while conserving mass, the undertray design lowers pressure beneath the car, enhances downforce, and maintains balance. This synergy of Venturi effect, Bernoulli's principle, and precise airflow management significantly improves stability and performance on track.

3.2 Performance of optimised Undertray at Different Ground Clearances

The results in table below shows that the optimized undertray performs consistently across different ground clearances, with minimal differences in drag and lift between 6.144 mm and 4.144 mm clearances. At higher speeds (28.5 m/s²), both clearances produced nearly identical drag and lift forces, indicating that small changes in ride height have little impact on aerodynamic performance at high speeds. At lower speeds (10 m/s²), the 4.144 mm clearance slightly increased drag and lift, enhancing the Venturi effect and downforce. Overall, the newly designed undertray remains effective and stable across various ride heights.

Simulations at ride heights of **6.144 mm** and **4.144 mm** showed the design performed consistently:

Speed (m/s)	Drag @6.144mm (N)	Lift @6.144mm (N)	Drag @4.144mm (N)	Lift @4.144mm (N)
10	2.70	-15.14	2.71	-15.17
15	6.08	-34.81	6.08	-34.82
20	10.78	-62.71	10.80	-62.95
28.5	21.90	-129.57	21.93	-129.60

Table 2 Performance numbers at 6.144 mm and 4.144 mm Ground Clearances

3.3 Discussion on Scaling and Wind Tunnel Testing

To validate the CFD results, a 1:5 scale undertray model was created and tested in a wind tunnel at speeds of 10 m/s, 15 m/s, and 20 m/s, using scaled ground clearances of 1.22 mm and 0.8 mm. The goal was to replicate real-world aerodynamic conditions.

3.3.1 Challenges in Scaling

Scaling presented notable challenges. The initial model lacked structural strength and had to be redesigned with thicker walls and reinforcements. However, matching aerodynamic behaviour proved difficult. Key fluid dynamics—like turbulence, flow separation, and boundary layer development—do not scale linearly, affecting accuracy.

Differences in Reynolds number between the scaled and full-size models also introduced inconsistencies in flow behaviour and downforce prediction.While the scaled tests offered valuable qualitative insights, they lacked precision in measuring aerodynamic forces. For accurate performance validation, full-scale CFD or wind tunnel testing is necessary, as small-scale models cannot fully replicate real driving conditions.

3.4 Ground Clearance and Test Speed

Wind tunnel tests were performed at two ground clearances 1.2 mm and 0.8 mm (scaled ground clearances) to assess the undertray's aerodynamic behavior. Results showed negative values, indicates lift rather than downforce, as noted by the test operator. Data was recorded every 5 seconds. Due to damage during the initial test, speeds were capped at 20 m/s in subsequent runs.

Speed (m/s)	Time (s)	Lift (N)	Drag (N)
10	0	-0.27	0.23
10	5	-0.27	0.23

10	10	-0.26	0.22
15	0	-0.47	0.46
15	5	-0.47	0.46
15	10	-0.48	0.47
20	0	-0.78	0.85
20	5	-0.80	0.87
20	10	-0.78	0.83

Table 3 :Drag vs lift test at 1.22 mm Ground Clearance

Speed (m/s)	Time (s)	Lift (N)	Drag (N)
10	0	-0.46	0.26
10	5	-0.46	0.25
10	10	-0.47	0.25
15	0	-0.82	0.48
15	5	-0.82	0.49
15	10	-0.81	0.49
20	0	-1.19	0.82
20	5	-1.20	0.81
20	10	-1.22	0.83

Table 4 :Drag vs lift test at 0.8 mm Ground Clearance

Tables 3 and 4 show that as speed increases, both lift and drag also rise. At 20 m/s, lift increased from -0.78 N (1.22 mm clearance) to -1.22 N (0.8 mm clearance), suggesting that higher ground clearance (1.22mm) slightly decreases lift without a major impact on drag. Also the unexpected high lift values may result from modifications made to the undertray for testing, particularly a slanted inlet, which could have altered airflow. Additionally, reduced clearance may have caused more turbulence, further contributing to the lift observed.

3.5 Pressure Test

Time (s)	kPa (1)	kPa (2)	kPa (3)	kPa (4)	kPa (5)	kPa (6)
Speed: 10 m/s						
0	-0.05	-0.10	-0.10	-0.10	-0.10	-0.11
2	-0.05	-0.10	-0.10	-0.10	-0.10	-0.11
4	-0.05	-0.10	-0.10	-0.10	-0.10	-0.11

6	-0.05	-0.10	-0.10	-0.10	-0.10	-0.11
8	-0.05	-0.10	-0.10	-0.10	-0.10	-0.11
10	-0.05	-0.10	-0.09	-0.10	-0.10	-0.10

Table 6 Pressure Test Results for 1.2 mm Ground Clearance at 10 m/s

Time (s)	**kPa(1)**	**kPa (2)**	**kPa (3)**	**kPa (4)**	**kPa (5)**	**kPa (6)**
Speed: 15 m/s						
0	**0.15**	**-0.23**	**-0.24**	**-0.26**	**-0.26**	**-0.23**
2	**-0.15**	**-0.22**	**-0.24**	**-0.26**	**-0.26**	**-0.24**
4	**-0.15**	**-0.24**	**-0.25**	**-0.26**	**-0.26**	**-0.24**
6	**-0.15**	**-0.24**	**-0.24**	**-0.26**	**-0.26**	**-0.25**
8	**-0.15**	**-0.24**	**-0.24**	**-0.26**	**-0.26**	**-0.25**
10	**-0.15**	**-0.24**	**-0.24**	**-0.26**	**-0.26**	**-0.24**

Table 7 Pressure Test Results for 1.2 mm Ground Clearance at 15 m/s

Time (s)	**kPa(1)**	**kPa (2)**	**kPa (3)**	**kPa (4)**	**kPa (5)**	**kPa (6)**
Speed: 20 m/s						
0	**-0.27**	**-0.41**	**-0.42**	**-0.45**	**-0.44**	**-0.41**
2	**-0.26**	**-0.40**	**-0.42**	**-0.45**	**-0.43**	**-0.41**
4	**-0.27**	**-0.41**	**-0.42**	**-0.45**	**-0.43**	**-0.40**
6	**-0.27**	**-0.41**	**-0.43**	**-0.45**	**-0.45**	**-0.41**
8	**-0.27**	**-0.41**	**-0.42**	**-0.45**	**-0.43**	**-0.41**

10	**-0.27**	**-0.41**	**-0.42**	**-0.45**	**-0.44**	**-0.41**

Table 8 Pressure Test Results for 1.2 mm Ground Clearance at 20 m/s

Time (s)	**kPa(1)**	**kPa (2)**	**kPa (3)**	**kPa (4)**	**kPa (5)**	**kPa (6)**
Speed: 10 m/s						
0	-0.05	-0.10	-0.10	-0.11	-0.11	-0.12
2	-0.05	-0.10	-0.10	-0.11	-0.11	-0.12
4	-0.05	-0.10	-0.10	-0.11	-0.11	-0.12
6	-0.05	-0.10	-0.10	-0.11	-0.11	-0.12
8	-0.05	-0.10	-0.10	-0.12	-0.12	-0.12
10	-0.05	-0.10	-0.10	-0.11	-0.11	-0.12

Table 9 Pressure Test Results for 0.8 mm Ground Clearance at 10 m/s

Time (s)	**kPa(1)**	**kPa (2)**	**kPa (3)**	**kPa (4)**	**kPa (5)**	**kPa (6)**
Speed: 15 m/s						
0	-0.10	-0.18	-0.20	-0.21	-0.23	-0.22
2	-0.10	-0.18	-0.20	-0.21	-0.22	-0.22
4	-0.10	-0.18	-0.20	-0.21	-0.22	-0.22
6	-0.10	-0.18	-0.20	-0.21	-0.22	-0.22
8	-0.10	-0.18	-0.20	-0.21	-0.22	-0.22
10	-0.10	-0.18	-0.20	-0.21	-0.22	-0.22

Table 10 Pressure Test Results for 0.8 mm Ground Clearance at 15 m/s

Time (s)	**kPa(1)**	**kPa (2)**	**kPa (3)**	**kPa (4)**	**kPa (5)**	**kPa (6)**
Speed: 20 m/s						
0	-0.18	-0.34	-0.38	-0.40	-0.40	-0.38
2	-0.18	-0.34	-0.37	-0.40	-0.40	-0.38
4	-0.18	-0.33	-0.38	-0.40	-0.40	-0.39
6	-0.18	-0.32	-0.37	-0.39	-0.39	-0.37
8	-0.18	-0.34	-0.38	-0.40	-0.40	-0.38
10	-0.18	-0.32	-0.38	-0.40	-0.39	-0.37

Table 11 Pressure Test Results for 0.8 mm Ground Clearance at 20 m/s

Wind tunnel tests with pressure taps at six points along the undertray compared two scaled models with ground clearances of 1.2 mm and 0.8 mm at speeds of 10, 15, and 20 m/s. Taps were positioned from the inlet through the convergent section to the diffuser exit to capture pressure distribution and recovery.

At higher speeds (15–20 m/s), the 1.2 mm model consistently showed more negative pressures at Taps 2–6, indicating stronger downforce and better flow attachment. For example, at 20 m/s, Tap 4 recorded −0.45 kPa, reflecting strong suction effects. The 0.8 mm model showed weaker negative pressures, higher variability, and signs of flow instability, limiting pressure recovery.

Overall, the 1.2 mm clearance delivered superior aerodynamic performance, with stable readings, greater negative pressure zones, and more effective pressure recovery.

3.6 Analysis of Real-World F1 Undertray Design and Simulation Constraints

The real-world Formula 1 undertray design was developed in alignment with the 2024 FIA Technical Regulations, ensuring compliance with strict dimensional and material rules. Key components such as the plank (made from Jabroc), floor body, fences, and diffuser were designed to meet these specifications, promoting both performance and fairness. The plank plays a vital role in controlling the car's ride height and center of gravity, while the rest of the undertray geometry is restricted to prevent aerodynamic advantages.

The CAD model (figure 24 and figure25) successfully integrated these regulatory requirements. However, a major limitation was encountered during simulation in ANSYS, due to the software's 500,000-node cap. Despite simplification efforts, the complexity of the undertray design exceeded this limit, making it impossible to carry out a full aerodynamic simulation. This constraint significantly affected the ability to validate the model's real-world aerodynamic performance.

Figure 25 CAD design of Formula One Undertray

IV. Conclusion

The study demonstrated that a 1.2 mm ground clearance offers superior aerodynamic performance over 0.8 mm, particularly at higher speeds. This is due to better airflow management and diffuser efficiency, resulting in enhanced downforce and vehicle stability. While both settings performed similarly at low speeds, 1.2 mm proved optimal for high-speed applications.When scaled to the BMM Formula Student vehicle, the corresponding effective ground clearance was calculated as 6.144 mm, offering the best balance between downforce and drag. The redesigned undertray improved airflow and reduced turbulence, though lower ride heights showed an increased risk of lift. The 1.2 mm setting offered the best compromise between stability and aerodynamic efficiency. Incorporating the 2024 FIA F1 Technical Regulations ensured that the undertray design adhered to real-world dimensional and material constraints, improving its practical relevance. A key limitation was the 500,000-node cap in ANSYS, which restricted full simulation and validation. This underlines the need for more advanced CFD tools or physical wind tunnel testing to comprehensively evaluate the design. In summary, the undertray design shows great potential but requires further validation through enhanced simulations and experimental testing to ensure peak performance in competitive motorsport environments.

ACKNOWLEDGEMENTS

I am grateful to Brunel University London for providing the resources and support for this project. My sincere thanks to Professor Timothy Minton for his invaluable guidance, and to Professor Kevin Robinson for his technical expertise and assistance with specialist testing. I also appreciate the encouragement of my colleagues and friends in the department, and the unwavering support of my family, which has been vital to my success.

REFERENCES

[1]. Anderson, J.D., 2017. *Computational Fluid Dynamics: The Basics with Applications*. McGraw-Hill Education.
[2]. AirShaper, 2020. Scale model wind tunnel testing explained. [online] airshaper.com. Available at: https://airshaper.com/videos/scale-model-wind-tunnel-testing/qqYiz1eo-F4.
[3]. Anon, (n.d.). *TecQuipment Subsonic Wind Tunnel – AF1300S – AYVA Educational Solutions*. [online] Available at: https://www.ayva.ca/eng/product/tecquipment-subsonic-wind-tunnel-af1300s/.
[4]. Ansys Learning Forum | Ansys Innovation Space, 2018. Limitations of ANSYS Student - Ansys Learning Forum | Ansys Innovation Space. [online] Available at: https://innovationspace.ansys.com/forum/forums/topic/limitations-of-ansys-student/ [Accessed 19 Sep. 2024].
[5]. Barlow, J.D., Rae, W.H., and Pope, A., 2020. *Low-Speed Aerodynamics: A Practical Guide*. Cambridge
[6]. University Press.
[7]. B.TecQuipment, 2020. *Subsonic Wind Tunnel 305 mm*. [online] Available at: https://www.tecquipment.com/subsonic-wind-tunnel-300mm-only.
[8]. Beranek, M., 2015. *Automotive Aerodynamics: The Basics of Automotive Aerodynamics*. Springer.
[9]. Bhatnagar, U., 2014. *Formula 1 Race Car Performance Improvement by Optimization of the Aerodynamic Relationship Between the Front and Rear Wings*.
[10]. Fédération Internationale de l'Automobile (FIA), 2024. *Formula One Technical Regulations*. Available at: FIA website [Accessed 19 September 2024].
[11]. Harris, R. and Waddington, C., 2018. Advances in Undertray Design for Formula Racing Cars. *International Journal of Vehicle Design*, 77(2), pp.139–158. Available at: ResearchGate [Accessed 19 September 2024].
[12]. Hu, T., 2023. Analysis of The Venturi Tunnel and Ground Effect. *Highlights in Science Engineering and Technology*, 38, pp.695–698. doi:https://doi.org/10.54097/hset.v38i.5933.
[13]. Houghton, E.L. and Carpenter, P.A., 2021. *Aerodynamics for Engineering Students*. CRC Press.
[14]. imeche, 2018. *Formula Student - Institution of Mechanical Engineers*. [online] Imeche.org. Available at: https://www.imeche.org/events/formula-student.
[15]. Katz, J., 2006. *Race Car Aerodynamics: Designing for Speed*. Cambridge, MA: R. Bentley.
[16]. Karl Eugene Jensen, 2011. *Aerodynamic Undertray Design for Formula SAE*.
[17]. Kuya, Y., Takeda, K. and Zhang, X., 2010. Computational Investigation of a Race Car Wing With Vortex Generators in Ground Effect. *Journal of Fluids Engineering*, 132(2). doi:https://doi.org/10.1115/1.4000741.
[18]. McLean, D., 2012. *Understanding Aerodynamics*. John Wiley & Sons.
[19]. Mohd, 2010. *Study of F1 Car Aerodynamics Front Wing Using Computational Fluid Dynamics (CFD)*.
[20]. Newey, A., 2020. *How To Build A Car: The Autobiography Of The World's Greatest Formula 1 Designer*. New York, USA: HarperCollins.
[21]. Pope, A., 2018. *Aerodynamics of Racing Cars: Theory and Application*. Springer.
[22]. Racecar Engineering, 2023. *Practical Guide to Aerodynamic Testing for Race Cars*. Racecar Engineering. Available at: Racecar Engineering website [Accessed 19 September 2024].
[23]. Smith, C., 2020. *The Physics of Racing: Understanding the Basics of Motorsport Engineering*. Elsevier.
[24]. Spalding, H., 2021. Ground Effect and the Evolution of Aerodynamics in Formula 1. *Journal of Motorsport History*, 35(2), pp.112–129. Available at: Elsevier [Accessed 19 September 2024].
[25]. White, F.M., 2018. *Fluid Mechanics*. McGraw-Hill Education.
[26]. Wright, R., 2018. *Formula 1: The Knowledge*. Haynes Publishing.
[27]. Zhang, X., Toet, W. and Zerihan, J., 2006. Ground Effect Aerodynamics of Race Cars. *Applied Mechanics Reviews*, 59(1), pp.33–49. doi:https://doi.org/10.1115/1.2110263.
[28]. Zaeed Ali Asgar S. Khokhar, 2015. Design and Analysis of Undertray Diffuser for a Formula Style Racecar. *International Journal of Research in Engineering and Technology*, 04(11), pp.202–210. doi:https://doi.org/10.15623/ijret.2015.0411035.
[29]. Z Anon, (n.d.). *TecQuipment Subsonic Wind Tunnel – AF1300S – AYVA Educational Solutions*. [online] Available at: https://www.ayva.ca/eng/product/tecquipment-subsonic-wind-tunnel-af1300s/.